Research in Astronomy and Astrophysics, 22:055013 (8pp), 2022 May https://doi.org/10.1088/1674-4527/ac5ee8

Photometric Investigation of Contact Binary DY Cet Based on TESS Data

M. F. Yıldırım[1,2]
[1] Çanakkale Onsekiz Mart University, Astrophysics Research Center and Ulupınar Observatory, 17020, Çanakkale, Turkey; mf.yildirim@hotmail.com
[2] Çanakkale Onsekiz Mart University, Department of Electricity and Energy, Çan Vocational School, 17400, Çanakkale, Turkey
Received 2022 January 2; revised 2022 March 1; accepted 2022 March 14; published 2022 April 29

Abstract

We present a photometric analysis of the Transiting Exoplanet Survey Satellite (TESS) light curve of contact binary system DY Cet and the behavior of its orbital period variation. The light curve and published radial velocity data analysis was performed using the Wilson–Devinney code. As a result of simultaneous analysis of the light curve with radial velocity data, the masses and radii of the system's components were determined as $M_1 = 1.55 \pm 0.02\ M_\odot$, $M_2 = 0.55 \pm 0.01\ M_\odot$ and $R_1 = 1.51 \pm 0.02\ R_\odot$, $R_2 = 0.95 \pm 0.02\ R_\odot$, respectively. The degree of contact (f) and mass ratio (q) of the system were determined as 23% and 0.355 ± 0.012, respectively. Orbital period analysis of DY Cet was conducted for the first time in this study. It was observed that the orbital period has a sinusoidal change with decreasing parabola. To explain the orbital period change, mass transfer between components is proposed with the assumption of conservative mass, and the transfer rate was calculated to be $dM/dt = 1.1 \times 10^{-7} M_\odot\ \mathrm{yr}^{-1}$. A possible third component is suggested for explaining the sinusoidal change, and the mass of the unseen component was determined as $0.13\ M_\odot$. The age of the DY Cet system was estimated as 3.77 Gyr.

Key words: stars: eclipsing binary stars – stars: fundamental parameters of stars – stars: individual (DY Cet)

1. Introduction

The minimum depths of W UMa type systems' light curves are equal or very close to each other. These systems are known as contact binary stars, according to the Kuiper (1941) classification. Later, contact systems with respect to Roche lobe geometry were reported on by Kopal (1955) and in this model, both stars were filled or even overflowed the inner Roche lobe. Therefore, the components are surrounded by a common envelope in most of the contact or overcontact W UMas. This indicates that the temperatures of the components are close to each other. The components of such systems are very close to each other. As a result, binary stars of the W UMa type are quite far from sphericity, due to the high gravitational perturbation forces they exert on each other. In this research, the sensitive Transiting Exoplanet Survey Satellite (TESS) light curve of the contact system DY Cet has been analyzed, together with the published radial velocity data to calculate the basic astrophysical parameters of the components. It also aims to analyze the orbital period change, which is not currently addressed in the literature.

DY Cet (Gaia DR2 5158131859934912640, TIC 441128066, 2MASS J02383318-1417565, HIP 12311, GSC 05291-00361, F5V) was determined to be an eclipsing binary system and included in the Hipparcos & Tycho catalogs (1997) as a W UMa type system. Using the Hipparcos light curve, some light elements of DY Cet were determined by Selam (2004). He ascertained the degree of contact of DY Cet as $f = 0.2$, the orbital inclination as $i = 77^\circ.5$ and the mass ratio as $q = 0.45$. The radial velocity of DY Cet was analyzed by Pribulla et al. (2009) and the orbital parameters of the system were calculated. The mass ratio of DY Cet as $q = 0.356(9)$ was determined by Pribulla et al. (2009), who estimated the spectral type as F5V. Pribulla et al. (2009) reported that the system DY Cet is an A sub-type W UMa. The light curve in the V filter of the system is given in the public data archive ASAS SN (Shappee et al. 2014; Kochanek et al. 2017). The spectroscopic study of the orbit of the system was done by Pourbaix et al. (2004). The light curve analysis of the system was performed with ASAS data by Deb & Singh (2011) and the basic astrophysical parameters of the component stars were determined. The normalized light curves from TESS data for DY Cet and many other eclipsing binary systems were obtained with the code written by Mortensen et al. (2021). These data can be accessed at the online address http://tessEBs.villanova.edu. There is no study of the orbital period change of DY Cet in the literature.

2. Data Information

Systems observed by the TESS satellite have been released and archived at the Mikulski Archive for Space Telescopes (MAST).[3] TESS observations of DY Cet began in October 2018 and were completed in November 2018. The data of the

[3] MAST, https://archive.stsci.edu.

Table 1
Minima Times of DY Cet (Equation (1) was Used for $O - C$ (days) Values)

HJD (2400000+)	Type	Method	Epoch	$O - C$ (days)	Reference
48500.2510	p	ccd	0	−0.0190	Hipparcos[a]
51427.1160	p	ccd	6640	0.0004	ROTSE (Paschke A.)[a]
51472.0800	p	ccd	6742	0.0038	VSOLJ No. 47
51472.0803	p	ccd	6742	0.0041	VSOLJ No. 55
51541.9459	s	ccd	6900.5	0.0045	VSOLJ No. 120
51541.9460	s	ccd	6900.5	0.0046	VSOLJ No. 47
51810.6150	p	ccd	7510	0.0121	BBSAG No. 55
51868.7900	p	ccd	7642	0.0028	Pojmanski G.[a]
52144.2810	p	ccd	8267	0.0001	Paschke Anton[a]
52194.0850	p	ccd	8380	−0.0052	VSOLJ No. 403
52576.0400	s	ccd	9246.5	0.0053	VSOLJ No. 721
53286.1540	s	ccd	10,857.5	0.0066	VSOLJ No. 1408
53322.0770	p	vis	10,939	0.0052	VSOLJ No. 43
53326.0470	p	vis	10,948	0.0081	VSOLJ No. 43
53337.7258	s	ccd	10,974.5	0.0059	IBVS No. 5843
53370.5634	p	ccd	11,049	0.0047	IBVS No. 5690
53402.5207	s	ccd	11,121.5	0.0047	IBVS No. 5677
53604.1828	p	ccd	11,579	0.0054	VSOLJ No. 44
53676.0307	p	ccd	11,742	0.0045	VSOLJ No. 44
53683.0830	p	vis	11,758	0.0042	VSOLJ No. 44
53683.0833	p	ccd	11,758	0.0045	VSOLJ No. 44
53994.9419	s	ccd	12,465.5	0.0042	IBVS No. 5806
54040.7832	s	ccd	12,569.5	0.0033	IBVS No. 5843
54048.0599	p	ccd	12,586	0.0070	VSOLJ No. 45
54130.9256	p	ccd	12,774	0.0041	VSOLJ No. 46
54802.0279	s	ccd	14,296.5	0.0037	VSOLJ No. 48
55543.6546	p	ccd	15,979	0.0012	IBVS No. 5960
55554.8941	s	ccd	16,004.5	0.0005	VSOLJ No. 51
55850.8857	p	ccd	16,676	0.0017	IBVS No. 6011
55881.9580	s	ccd	16,746.5	−0.0017	VSOLJ No. 53
56287.9284	s	ccd	17,667.5	0.0011	VSOLJ No. 55
56596.0396	s	ccd	18,366.5	0.0001	VSOLJ No. 56
56601.9909	p	ccd	18,380	0.0007	VSOLJ No. 56
56603.9772	s	ccd	18,384.5	0.0034	VSOLJ No. 56
56614.9942	s	ccd	18,409.5	0.0007	VSOLJ No. 56
56955.0647	p	ccd	19,181	0.0017	VSOLJ No. 59
56976.0016	s	ccd	19,228.5	0.0011	VSOLJ No. 59
57309.0211	p	ccd	19,984	0.0037	VSOLJ No. 61
57353.9786	p	ccd	20,086	0.0007	VSOLJ No. 61
57724.9040	s	ccd	20,927.5	0.0013	VSOLJ No. 63
57741.8740	p	ccd	20,966	0.0009	VSOLJ No. 63
58038.0849	p	ccd	21,638	0.0009	VSOLJ No. 64
58779.0508	p	ccd	23,319	−0.0012	VSOLJ No. 67
58779.0528	p	ccd	23,319	0.0008	VSOLJ No. 67
58820.9232	p	ccd	23,414	−0.0039	VSOLJ No. 67
58820.9239	p	ccd	23,414	−0.0032	VSOLJ No. 67
58820.9250	p	ccd	23,414	−0.0021	VSOLJ No. 67
58820.9260	p	ccd	23,414	−0.0011	VSOLJ No. 67
58411.2128	s	TESS	22,484.5	0.0000	Present Paper
58411.4336	p	TESS	22,485	0.0004	Present Paper
58417.1637	p	TESS	22,498	0.0003	Present Paper
58417.3836	s	TESS	22,498.5	−0.0002	Present Paper
58421.3507	s	TESS	22,507.5	−0.0002	Present Paper
58421.5714	p	TESS	22,508	0.0001	Present Paper
58428.1831	p	TESS	22,523	−0.0001	Present Paper
58428.4037	s	TESS	22,523.5	0.0001	Present Paper
58848.9143	s	ccd	23,477.5	−0.0029	VSOLJ No. 67
58848.9152	s	ccd	23,477.5	−0.0020	VSOLJ No. 67

Table 1
(Continued)

HJD (2400000+)	Type	Method	Epoch	$O-C$ (days)	Reference
58848.9164	s	ccd	23,477.5	−0.0008	VSOLJ No. 67
58848.9172	s	ccd	23,477.5	0.0000	VSOLJ No. 67
59073.2725	s	ccd	23,986.5	−0.0068	VSOLJ No. 69
59073.2745	s	ccd	23,986.5	−0.0048	VSOLJ No. 69
59073.2746	s	ccd	23,986.5	−0.0047	VSOLJ No. 69
59073.2756	s	ccd	23,986.5	−0.0037	VSOLJ No. 69
59077.2411	s	ccd	23,995.5	−0.0053	VSOLJ No. 69
59077.2415	s	ccd	23,995.5	−0.0049	VSOLJ No. 69

Note.
[a] The data from $O-C$ gateway, http://var2.astro.cz/ocgate/ocgate.php?star=dy+cet.

system given in Sector 4 with 120 s exposure time were used in the observations. The data downloaded from the TESS data archive were first converted to luminosity and then converted to normalized flux based on the 0.25 phase. The minima times were used to examine the orbital period change of DY Cet. For this purpose, the minima times of the selected contact system were collected from the literature and were calculated from the light curves generated from the TESS satellite data. The eclipse times of the system were obtained by the least squares method with a written code. Minima times calculated from TESS data are converted from Barycentric Julian Date (BJD) to Heliocentric Julian Date (HJD). The list of minima times obtained from satellite data is listed in Table 1. Eight minima times were obtained from the satellite data. It has been seen that the errors of the calculated minima times are in the range of about 8–18 s. All minima times of DY Cet used in orbital period analysis are listed in Table 1. Published minima times were compiled from the "$O-C$ Gateway" (Paschke & Brat 2006) database. The orbital period analysis study of the system was carried out with a total of 66 minima times, including 3 visual, 55 CCD and 8 TESS minima times (35 of these minima times are the first and 31 of them are the second minima times) (see Table 1).

3. Simultaneous Analysis of Light Curve with Radial Velocity Data

The light curve of the DY Cet system, taken from the TESS database and the radial velocity data of the components from the literature (Pribulla et al. 2009), were analyzed. In this study, the Wilson–Devinney (WD) method, which is widely known and preferred in the literature, was used (Wilson 1990, 1993; van Hamme & Wilson 2003). We utilized the 2003 version (van Hamme & Wilson 2003) of the WD code (Wilson & Devinney 1971). While calculating the theoretical light and radial velocity curves, the free parameters (mass ratio (q), orbital inclination (i), surface potentials ($\Omega_{1,2}$), fractional luminosity contributions of the primary component (L_1) and effective temperature of the second component (T_2)) were chosen according to the characteristics of the selected system. The gravity-darkening coefficient of the components was taken as $g_1 = g_2 = 0.32$ (Lucy 1967) and the bolometric albedos as $A_1 = A_2 = 0.5$ (Rucinski 1969). In this study, Cox (2000)'s recommended value of 6650 K was applied according to the FV5 spectral type determined by Pribulla et al. (2009) as the effective temperature (T_1) of the first component.

When employing the WD method, MOD selection is made according to the shape of the light curve and the characteristics of the system. MOD3 is preferred for systems where the surface potential values of the components exceed the critical potential value. In this paper, MOD3 was also used for the contact system DY Cet. The results obtained from the simultaneous solution of the light and radial velocity curves, together with the results published in the literature, are expressed in Table 2. Observational and theoretical light curves are displayed in Figure 1, and the compatibility of the radial velocity curves of the star with the theoretical curves is demonstrated in Figure 2.

4. Orbital Period Change

Since observed minus calculated ($O-C$) analysis serves as an important tool in our understanding of the nature of stars, this method of analysis has been used by many authors (e.g., Soydugan et al. 2011; Yıldırım et al. 2019). The sources of period variation in binary stars are mostly mass, angular momentum transfer and loss, third-body effect, magnetic activity and apsidal motion. Whether there is the period change of whatever character, it can be understood with $O-C$ graphs created using the minima times. For the DY Cet system, when the $O-C$ graph is examined in the $O-C$ Atlas prepared for binary stars (Kreiner 2004), it is seen that the period change is in the form of a decreasing parabola and above it a sinusoidal wave. Therefore, it was decided to analyze the orbital period change of DY Cet. For this, by adding TESS satellite data to the minima times collected from the literature, $O-C$ data were calculated and prepared for analysis. Analysis was performed

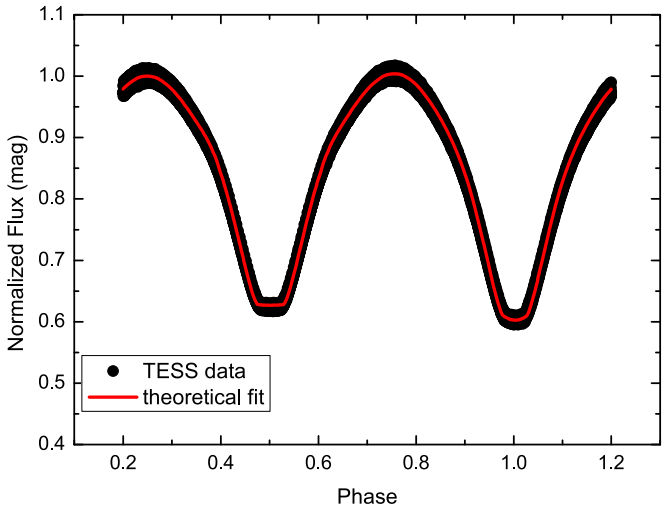

Figure 1. Comparison of TESS light curve of the DY Cet system with light curve obtained from the theoretical model.

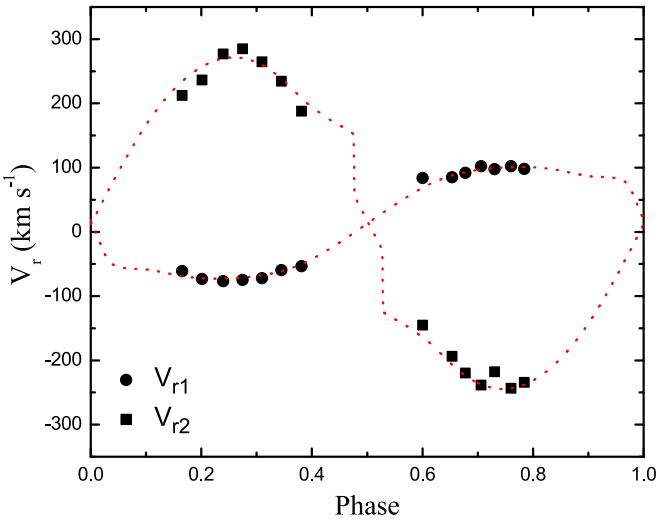

Figure 2. Comparison of observational and theoretical radial velocity curves of components of the DY Cet system.

Table 2
Comparison of Light and Radial Velocity Curves of the DY Cet System with Results in the Literature

Parameter	Deb & Singh (2011)	This Study
T_0 (HJD+2400000)	⋯	48,500.2511 (9)
P (days)	0.440,790	0.440,793,5 (1)
i (°)	82.48 (34)	85.6 (2)
T_1 (K)	6650 (178)	6650[a]
T_2 (K)	6611 (176)	6600 (30)
$\Omega_1 = \Omega_2$	2.529 (5)	2.523 (11)
q	0.356	0.355 (12)
a ($R_\odot$)	3.046 (27)	3.13 (5)
V_γ (km s^{-1})	⋯	14 (5)
$A_1 = A_2$	0.5	0.5
$g_1 = g_2$	0.32	0.32
$l_1/(l_1 + l_2)$	⋯	0.721 (12)
$l_2/(l_1 + l_2)$	⋯	0.279
l_3	0	0
r_1 (pole)	⋯	0.4522 (7)
r_1 (side)	⋯	0.4865 (8)
r_1 (back)	⋯	0.5163 (4)
r_2 (pole)	⋯	0.2839 (5)
r_2 (side)	⋯	0.2973 (3)
r_2 (back)	⋯	0.3383 (6)
f (%)	24	23

Note.
[a] T_1 was determined from the spectral type.

by giving weighted values of 10 for ccd and TESS data and 1 for visual data. First, the minima times were calculated using Equation (1) to represent the parabolic change of DY Cet in the $O - C$ graph

$$\mathrm{HJD(MinI)} = T_0 + E \times P + Q \times E^2, \quad (1)$$

where T_0 is the initial primary minimum, E the epoch number, P period and Q denotes the coefficient of the parabolic term. Q is positive if the period of the system is increasing and negative if it is decreasing. Equation (2) is used to express the change in period per unit time

$$\frac{\Delta P}{P} = \frac{2Q}{P}. \quad (2)$$

If the mass transfer is conservative, using Kepler's third law, the following relation can be obtained between the period change (ΔP) and the amount of mass transferred ($\dot{m}_1$) (Kwee 1958)

$$\frac{\Delta P}{P} = \frac{3\dot{m}_1(m_1 - m_2)}{m_1 m_2} = \frac{3(1 - q^2)\dot{m}_1}{qM}. \quad (3)$$

In Equation (3), m_1 and m_2 are the masses of the components, M is the total mass of the system, and q ($=m_2/m_1$) is the mass ratios of the components. The most basic statement for modeling the sinusoidal changes seen in $O - C$ graphs using the possible third-body induced LITE was given by Irwin (1959) and Mayer (1990)

$$\triangle t = \frac{a_{12}\sin i'}{c}\left\{\frac{1 - e'^2}{1 + e'\cos\nu'}\sin(\nu' + \omega') + e'\cos\omega'\right\}. \quad (4)$$

The Δt value is the time delay due to a possible third object. In Equation (4), c expresses the speed of light, a_{12} the semimajor axis length of the third possible component orbit, i' orbital inclination, e orbital eccentricity, v' true anomaly and w' the longitude value of the periastron of the third-body orbit. In this case, the light elements of DY Cet follow

$$\mathrm{HJD(MinI)} = T_0 + E \times P + Q \times E^2 + \triangle t. \quad (5)$$

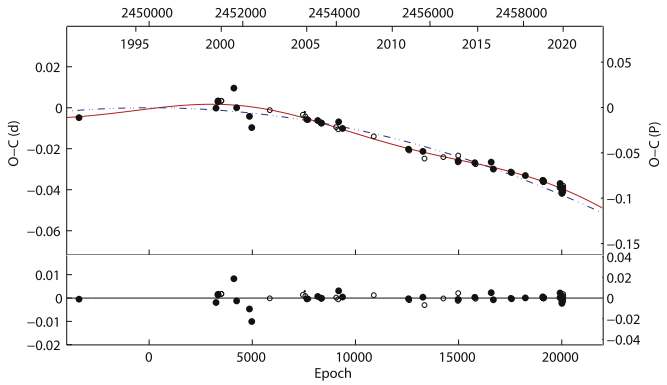

Figure 3. Distribution of $O-C$ data of DY Cet and its representation with theoretical curves. The dashed line is parabolic (dashed blue lines), and the continuous red line is the theoretical curves calculated using the parabolic terms and LITE together. The bottom panel shows differences from the theoretical curve.

$O-C$ changes due to magnetic cycling are cyclical and can be represented by the following relation

$$\mathrm{HJD(MinI)} = T_0 + E \times P + Q \times E^2 + A_{\mathrm{mod}} \sin\left[\frac{2\pi}{P_{\mathrm{mod}}}(E - T_s)\right]. \quad (6)$$

In Equation (6), A_{mod}, P_{mod} and T_s represent the semi-amplitude, period of sinusoidal changes and minimum time of sinusoidal change, respectively. $O-C$ analysis was performed by combining the eight minima times obtained from the TESS satellite data of the DY Cet system with the minima times collected from the literature. Using 66 minima times, $O-C$ analysis was performed with the distribution of data spanning approximately 30 yr (mostly CCD data, see Table 1).

First, Equation (1) was applied to represent the $O-C$ data of the system. Taking the differences of the observational data from the theoretical curve obtained, it was observed that there is a sinusoidal change in the residuals (see Figures 3 and 4). Therefore, it was taken into account that the $O-C$ variation of the system is both parabolic and sinusoidal. The source of sinusoidal period change could be an active component in the binary (magnetic activity) or a third body in the system. First, considering the third body probability, the $O-C$ change was modeled using the parabolic terms and light-time effect (LITE, Equation (5)), and the determined parameters are listed in Table 3 with their errors. In this table, some orbital parameters and the minimum mass value (approximately 0.13 $M_\odot$) of the possible third body are also provided. The orbital period of the possible third component around the common center of mass of the system was calculated as approximately 6939 days. The reason for the decrease in the period is suggested as inter-component mass transfer, and this ratio was calculated as $dM/dt = 1.1 \times 10^{-7}\ M_\odot\ \mathrm{yr}^{-1}$. The rate of decrease in the period was determined as $dP/dt = 1.75 \times 10^{-7}$ day yr^{-1}.

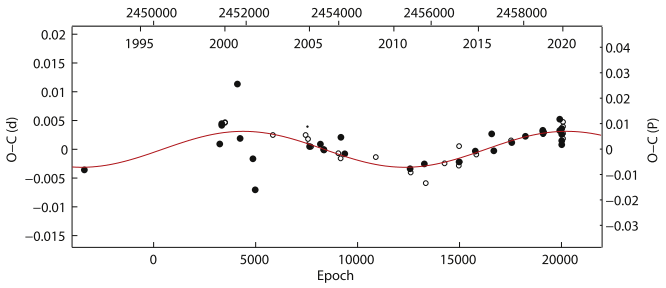

Figure 4. Cyclic change of $O-C$ data for DY Cet and its representation with theoretical curve (continuous line) calculated using LITE.

Table 3
Parameters and their Errors Obtained from $O-C$ Analysis for DY Cet

Parameter	Value
To (HJD+2400000)	48,500.2511 (9)
P_{orb} (days)	0.440,793,5 (1)
Q (days)	1.1 (1) $\times 10^{-10}$
dP/dt (day yr^{-1})	1.75×10^{-7}
dM/dt ($M_\odot$ yr^{-1})	1.1×10^{-7}
a_{12} sin i (AB)	0.54 (8)
e	0[a]
ω (deg)	90[a]
A_3 (day)	0.0031 (6)
T' (HJD+2400000)	53,289 (166)
P_{12} (yr)	19 (3)
$f(m_3)$ ($M_\odot$)	0.0004 (1)
m_3 ($M_\odot$) (for $i = 90°$)	0.13

Note.
[a] Adopted.

The Applegate model of magnetic activity also assumes changes in the brightness of the system in the same course as $O-C$ changes and changes the color of the system to blue when the system is in the brightest state. The cyclical change seen in the $O-C$ graph of DY Cet may also be due to possible magnetic activity of the primary component of DY Cet, which is a cool star having a convective outer envelope. Therefore, Equation (6) was applied to the $O-C$ data to represent the cyclical changes with the parabolic term as well. The cyclic variation parameters found are listed in Table 4. In order to produce such a cyclic period change, the subsurface magnetic field value of the relevant component should be on the order of 6.3 kG. Also, for the primary component to produce such a cyclic orbital period change, the differential rotational variation must be on the order of 0.0004.

5. Discussion and Results

The most sensitive photometric data available to date, namely, the TESS light curve, were analyzed together with the published radial velocity data to determine the basic

Table 4
Applegate Model Parameters for DY Cet

Parameter	Value
$P_{\rm mod}$ (yr)	19
$\Delta P/P$	2.8×10^{-6}
ΔJ (erg s^{-1})	1.5×10^{47}
$\Delta\Omega/\Omega$	0.0004
ΔE (erg)	1.9×10^{40}
I_s (g cm^2)	2.3×10^{54}
$\Delta L/L_1$	0.006
B (kG)	6.3
ΔQ_1	4.5×10^{49}
ΔQ_2	1.6×10^{49}

Table 5
Basic Physical Parameters of DY Cet and Comparison with Study of Deb & Singh (2011)

Parameter	Deb & Singh (2011)	This Study
M_1 ($M_\odot$)	1.436 (34)	1.55 (2)
M_2 ($M_\odot$)	0.511(25)	0.55 (1)
R_1 ($R_\odot$)	1.408 (14)	1.51 (2)
R_2 ($R_\odot$)	0.938 (10)	0.95 (2)
log g_1 (cgs)	⋯	4.27 (1)
log g_2 (cgs)	⋯	4.22 (2)
$M_{\rm bol,1}$ (mag)	⋯	3.24 (15)
$M_{\rm bol,2}$ (mag)	⋯	4.28 (17)
L_1 ($L_\odot$)	3.840 (482)	3.95 (13)
L_2 ($L_\odot$)	1.507 (194)	1.55 (25)
BC_1	⋯	0.077
BC_2	⋯	0.022
$d_{\rm photometry}$ (pc)	⋯	210 (16)
$d_{\rm Gaia\text{-}EDR3}$ (pc)	⋯	186.9 (5)

astrophysical parameters and system properties of DY Cet. Using the parameters determined as a result of the analysis, with the assistance of basic astrophysical relations, the basic astrophysical parameters of the system were calculated and are given in Table 5. In this study, the masses and radii of the component stars were calculated as $M_1 = 1.55 \pm 0.02$ $M_\odot$, $M_2 = 0.55 \pm 0.01$ $M_\odot$ and $R_1 = 1.51 \pm 0.02$ $R_\odot$, $R_2 = 0.95 \pm 0.02$ $R_\odot$, which are slightly different from the results of Deb & Singh (2011). The solar values ($T_{\rm eff} = 5771.8 \pm 0.7$ K, $M_{\rm bol} = 4.7554 \pm 0.0004$ mag, $g = 27423.2 \pm 7.9$ cm s^{-2}), referenced from Pecaut & Mamajek (2013), were used in the computations. Bolometric correction (BC) values given by Eker et al. (2020) were utilized to calculate the bolometric brightness of the components of the system (see Table 5). In addition, the temperatures determined for the components were found to be different from the last light curve analysis performed in the literature (see Table 2). As a result of the analysis, the temperature gap between the components was determined to be approximately $\Delta T = 50$ K. The mass ratio of DY Cet was calculated as $q = 0.355$ (12) and the degree of contact (f) was calculated as 23%. As a result of the photometric analysis of DY Cet, its distance was determined as $d = 210 \pm 16$ pc and this value was found to be close to the value of Gaia Collaboration (2020) ($d_{\rm Gaia} = 186.9 \pm 5$), to the order of 2σ.

It is very important to determine the age of contact systems. Various methods have been presented for the age determination of contact systems (e.g., Bilir et al. 2005; Yıldız 2014). In this study, the age of DY Cet was calculated as 3.77 Gyr using the calculation method proposed by Yıldız (2014) and applied by Latkovic et al. (2021). Bilir et al. (2005) calculated the kinematic age for W UMas as about 5.47 Gyr. The mean age values for A and W subtypes of contact systems were found by Yıldız (2014) as 4.4 and 4.6 Gyr, respectively, which support the age value of DY Cet calculated in this study.

To examine the period change, eight minima times were calculated from the light curve obtained from the TESS satellite data (see Table 1). Since these minima times are precisely determined and the total minimum time of the system is not excessive, it is eminently suitable for $O-C$ analysis. The orbital period analysis of DY Cet was carried out for the first time. It was determined that the orbital period of the system has decreased. As the reason for this decrease (assuming conservative mass), mass transfer from the more massive component to the less massive one has been proposed. The rate of decrease in the period was calculated as $dP/dt = 1.52$ s century^{-1} and the mass transfer rate was found to be $dM/dt = 1.1 \times 10^{-7} M_\odot$ yr^{-1}. The cyclical change of DY Cet in the $O-C$ graph was first explained by a possible third object. The minimum mass value of the unseen component is 0.13 $M_\odot$, and the period of the possible third component was determined as 19 yr.

The second reason for the cyclical change in the $O-C$ distribution may be the magnetic activity of the components. The X-ray flux of the DY Cet system was measured by Chen et al. (2006) and this possibility should also be taken into account. When Table 4 is examined, it is seen that there are values close to the parameter ranges predicted by Applegate (1992). However, the quadrupole moment of the components (changes in the star's quadrupole moment are transferred to the orbital period due to spin-entanglement locking) was calculated as approximately 10^{49} g cm^2 for both components (see Table 4). The equation $\Delta P/P = -9\Delta Q/Ma^2$ proposed by Lanza & Rodono (2002) was utilized to calculate the quadrupole moment of the components. It was reported by Lanza & Rodono (1999) that this value should be approximately 10^{51}–10^{52} g cm^2 for close eclipsing binary systems indicating magnetic cycles. In addition, it was stated by Lanza (2006) that it would not be sufficient to explain the orbital period modulations of the components by the convective outer envelopes, according to the Applegate (1992) model. Therefore, the existence of a third component (possibly an M dwarf) comes to the fore to explain the periodic $O-C$ change of the DY Cet system. Therefore, analyses should be updated to test

Table 6
Some Contact Systems Close to the Degree of Contact value for DY Cet

System	Period (days)	Degree of Contact (f; % as)	Spectral Type	ΔT (K)	$O-C$ Change Type	Reference
DX Tuc	0.377,107,8 (1)	14.9 (2)	F7IV/V (3)	68 (2)	Downward Par. (1)	(1), (2), (3)
U Peg	0.374,777,8 (1)	15 (4)	G2IV (4)	75 (4)	Downward Par.+ Cyclical (1)	(1), (4)
V1128 Tau	0.305,370,2 (1)	14.70 (5)	F8V (6)	269 (5)	Downward Par.+ Cyclical (1)	(1), (5), (6)
SS Ari	0.405,975,5 (1)	18 (7)	G0 (8)	284 (7)	Downward Par.+ Cyclical (1)	(1), (7), (8)
VZ Lib	0.358,253,6 (1)	19.40 (2)	G7 (2)	210 (2)	Downward Par. (1)	(1), (2)

References. (1): Kreiner (2004), (2): Szalai et al. (2007), (3): Selam (2004), (4): Pribulla & Vanko (2002), (5): Zhang et al. (2011), (6): Rucinski et al. (2008), (7): Kim et al. (2003), (8): Yang (2011).

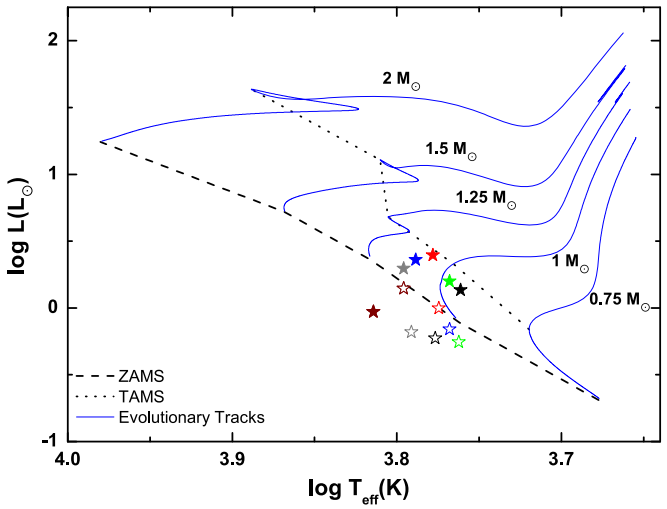

Figure 5. log $T_{\rm eff}$–log L graph representation of the first and second components of DY Cet (red), VZ Lib (black), SS Ari (blue), U Peg (green), V1128 Tau (brown) and DX Tuc (gray) systems. (The first components of the systems are displayed as filled stars and the second components as hollow stars). Evolutionary paths, and ZAMS and TAMS lines were created according to the MIST single star model in solar chemical abundance.

for this unseen possible component using different data, primarily high-resolution spectra of the system.

Some information about the five contact systems close to the degree of contact of DY Cet is given in Table 6. In addition, the temperature gap between the components of these systems is close to DY Cet. It was observed that all of the selected systems have decreasing orbital periods, similar to DY Cet. The systems listed in Table 6 together with DY Cet are plotted on the log $T_{\rm eff}$–log L graph (see Figure 5). Evolutionary pathways and zero age main sequence (ZAMS) and terminal age main sequence (TAMS) lines have been created based on MIST models in single stars and Sun chemical abundance (Paxton et al. 2011, 2013, 2015; Choi et al. 2016; Dotter 2016) (for the metallicity Z [Fe/H] = 0.014). In Figure 5, the primary component of DY Cet is close to the TAMS line, while the second component is located close to the ZAMS line. The primary components of VZ Lib, SS Ari, U Peg and DX Tuc are located on the main sequence, while the secondary components are located under the ZAMS line. Unlike most contact systems, the first component of V1128 Tau exhibits lower luminosity relative to its temperature.

DY Cet may come into thermal equilibrium by taking into account the low temperature difference of the components and the decrease in orbital period. Therefore, it is important to follow and test the behavior of the orbital period change of DY Cet in the future. To better understand the nature of DY Cet, satellite observations and spectral observations are needed to identify the possible third component in the system.

Acknowledgments

We thank the referee for her suggestions and contributions. For his support and contributions, we would like to thank Dr. Faruk SOYDUGAN. We thank Dr. Theodor Pribulla for sharing the radial velocity data with us. In this paper, Gaia-EDR3 data of the Gaia mission were used (https://www.cosmos.esa.int/gaia). In this study, data collected by the TESS mission were taken and used from the public data archive MAST (https://archive.stsci.edu). We thank the TESS and Gaia teams for the data used in this research. The VIZIER and SIMBAD databases at CDS in Strasbourg, France were used in this paper.

References

Applegate, J. H. 1992, ApJ, 385, 621
Bilir, S., Karataş, Y., Demircan, O., & Eker, Z. 2005, MNRAS, 357, 497
Chen, W. P., Sanchawala, K., & Chiu, M. C. 2006, AJ, 131, 990
Choi, J., Dotter, A., Conroy, C., et al. 2016, ApJ, 823, 102
Cox, A. N. 2000, Allen's Astrophysical Quantities (4th ed.; New York: AIP Press)
Deb, S., & Singh, H. P. 2011, MNRAS, 412, 1787
Dotter, A. 2016, ApJS, 222, 8
Eker, Z., Soydugan, F., Bilir, S., et al. 2020, MNRAS, 496, 3887
Gaia Collaboration 2020, yCat
Irwin, J. B. 1959, AJ, 64, 149
Kim, C. H., Lee, J. W., Kim, S. L., et al. 2003, AJ, 125, 322
Kochanek, C. S., Shappee, B. J., Stanek, K. Z., et al. 2017, PASP, 129, 980
Kopal, Z. 1955, AnAp, 18, 379
Kreiner, J. M. 2004, AcA, 54, 207
Kuiper, G. P. 1941, AJ, 93, 133
Kwee, K. K. 1958, BAN, 14, 131
Lanza, A. F. 2006, MNRAS, 369, 1773
Lanza, A. F., & Rodono, M. 1999, A&A, 349, 887

Lanza, A. F., & Rodono, M. 2002, AN, 323, 424
Latkovic, O., Ceki, A., & Lazarevic, S. 2021, MNRAS, 254, 18
Lucy, L. B. 1967, ZA, 65, 89
Mayer, P. 1990, BAICz, 41, 231
Mortensen, D., Eisner, N., IJspeert, L., et al. 2021, BAAS, 53, 1
Paschke, A., & Brat, L. 2006, OEJV, 23, 13
Paxton, B., Bildsten, L., Dotter, A., et al. 2011, ApJS, 192, 3
Paxton, B., Cantiello, M., Arras, P., et al. 2013, ApJS, 208, 4
Paxton, B., Marchant, P., Schwab, J., et al. 2015, ApJS, 220, 15
Pecaut, M. J., & Mamajek, E. E. 2013, ApJS, 208, 9
Pourbaix, D., Tokovinin, A. A., Batten, A. H., et al. 2004, AA, 424, 727
Pribulla, T., & Vanko, M. 2002, CAOSP, 32, 79
Pribulla, T., Rucinski, S. M., Blake, R. M., et al. 2009, AJ, 137, 3655
Rucinski, S. M. 1969, AcA, 19, 245
Rucinski, S. M., Pribulla, T., Mochnacki, S. W., et al. 2008, AJ, 136, 586
Selam, S. O. 2004, A&A, 416, 1097
Shappee, B. J., Prieto, J. L., Grupe, D., et al. 2014, AJ, 788, 13
Soydugan, E., Soydugan, F., Şenyu¸z, T., et al. 2011, NewA, 16, 72
Szalai, T., Kiss, L. L., Meszaros, S. Z., et al. 2007, A&A, 465, 943
The Hipparcos and Tycho catalogues 1997, ESA SP Series, 1200
van Hamme, W., & Wilson, R. E. 2003, ACP, 298, 323
Wilson, R. E. 1990, AJ, 356, 613
Wilson, R. E. 1993, ASP, 38, 91
Wilson, R. E., & Devinney, E. J. 1971, ApJ, 166, 605
Yang, Y. G. 2011, RAA, 11, 181
Yıldırım, M. F., Aliçavuş, F., & Soydugan, F. 2019, RAA, 19, 1
Yıldız, M. 2014, MNRAS, 437, 185
Zhang, X. B., Ren, A. B., Luo, C. Q., & Luo, Y. P. 2011, RAA, 11, 583